Climate Dynamics (1996) 12:535–544

Climate Dynamics

Redistribution of sea level rise associated with enhanced greenhouse warming: a simple model study

William W. Hsieh[1] and Kirk Bryan[2]

[1] Department of Oceanography, University of British Columbia, Vancouver, BC, Canada V6T 1Z4
[2] GFDL/NOAA, Princeton, NJ 08540, USA

Received: 10 March 1995 / Accepted: 18 December 1995

Abstract. Future sea level rise from thermal expansion of the World Ocean due to global warming has been explored in several recent studies using coupled ocean-atmosphere models. These coupled models show that the heat input by the model atmosphere to the ocean in such an event could be quite non-uniform in different areas of the ocean. One of the most significant effects predicted by some of the models is a weakening of the thermohaline circulation, which normally transports heat poleward. Since the greatest heat input from enhanced greenhouse warming is in the higher latitudes, a weakening of the poleward heat transport effectively redistributes the heat anomaly and the associated sea level rise to lower latitudes. In this study, the mechanism of ocean circulation spindown and heat redistribution was studied in the context of a much simpler, linearized shallow water model. Although the model is much simpler than the three-dimensional ocean circulation models used in the coupled model experiments, and neglects several important physical effects, it has a nearly 10-fold increase in horizontal resolution and clearer dynamical interpretations. The results indicated that advanced signals of sea level rise propagated rapidly through the action of Kelvin and Rossby waves, but the full adjustment toward a more uniform sea level rise took place much more slowly. Long time scales were required to redistribute mass through narrow currents trapped along coasts and the equatorial wave guide. For realistic greenhouse warming, the model showed why the sea level rise due to ocean heating could be far from uniform over the globe and hence difficult to estimate from coastal tide gauge stations.

1 Introduction

This study is concerned with future sea level rise from thermal expansion of the ocean associated with global greenhouse warming. It follows the work by Bryan (1996) who used a coupled GCM (basically that of Manabe et al. 1991) to study the effects of increasing atmospheric carbon dioxide on global sea level. In the main experiment of Bryan (1996), atmospheric carbon dioxide was increased at the rate of 1%/year for 100 years. In another experiment, atmospheric carbon dioxide was decreased 1%/year, and a third experiment was a control run in which the atmospheric carbon dioxide level was kept constant. The regions of largest heat influx into the ocean were the subpolar North Atlantic and the Southern Ocean. As heating anomalies were greatest in subpolar latitudes, this led to a weakening of the ocean thermohaline circulation. Changes in thermohaline circulation caused a redistribution of heat within the ocean from high latitudes to the equator, producing a more uniform sea level rise than would have occurred otherwise. In this study, the ocean circulation spindown and heat redistribution were studied using a much simpler shallow water model, which was able to provide insights on the mechanisms and timescale of this redistribution process, and thereby complement the coupled GCM study of Bryan (1996). For a literature review on modeling the sea level rise problem, see Bryan (1996) and Warrick and Oerlemans (1990).

The adjustment of the global sea level to a heat input at given latitudes can be viewed as a modified Rossby adjustment problem. Two experiments with simple ocean models were run to study the adjustment of the world ocean to gradually increasing sea level in (a) the northern North Atlantic and in (b) the Southern Ocean, these being the main regions of surface heat flux into the ocean under global warming as found by Bryan (1996).

The purposes of running these simple ocean models in addition to the coupled model were as follows: (1) In the coupled GCM, the ocean resolution of 4.5° latitude by 3.75° longitude, being an order of magnitude larger than the mid-latitude ocean's internal Rossby radius, was far too coarse to properly resolve the coastal Kelvin wave (Hsieh et al. 1983), a major player in

Correspondence to: W. W. Hsieh

the Rossby adjustment problem with side boundaries. At this resolution, even the equatorial Kelvin wave was ill-resolved (O'Brien and Parham 1992; Ng and Hsieh 1994). These coarse resolution models would give inaccurate transports along the continental margins and along the equator, possibly yielding inaccurate global sea level distribution. By using simple shallow water models, we were able to run higher resolution studies with 1/3 degree resolution in both latitude and longitude. (2) The simple Rossby adjustment study with a linear shallow water model allowed us to identify separately the effects due to sources in the northern North Atlantic and in the Southern Ocean. The simpler dynamics also facilitated relating the observed model behavior to various wave phenomena and other simple theories (e.g., Stommel and Arons 1960a, b; Kawase 1987).

2 Numerical experiments with a shallow-water model

Shallow-water models have been extensively used to model the response of the thermocline to wind, particularly in problems associated with El Niño in the Equatorial Pacific (Philander 1990). It is easiest to visualize the upper ocean as an active layer of uniform density ρ_1, over a deep inactive layer of greater density ρ_2. The linearized form of the governing equations are exactly like the classical ocean tidal equations except that gravity is multiplied by a small factor $\gamma=(\rho_2-\rho_1)/\rho_1$.

The linearized shallow water equations used in the present model are:

$$\partial_t \boldsymbol{u} + f\boldsymbol{k}\times\boldsymbol{u} + g\gamma\nabla h = -\mu\boldsymbol{u} \tag{1}$$

and

$$\partial_t h + \overline{h}\nabla\cdot\boldsymbol{u} = q, \tag{2}$$

where $\boldsymbol{u}=(u,v)$ is the horizontal velocity vector, $\boldsymbol{k}$ is the local vertical unit vector, f is the Coriolis parameter, g is the acceleration of gravity, h is the perturbation of the upper layer thickness from $\overline{h}$, the background upper layer thickness, which is assumed to be constant, and q is a source term for upper layer thickness perturbation, due to the effects of surface heating. All frictional forces are assumed to be given by a linear drag law with a drag coefficient of μ.

Applying such a model to study the mass adjustment of the thermocline to surface heating is a drastic simplification. The key assumption is that there is no interaction between the background circulation and the adjustment process. More details are given in the Appendix.

Alternatively, the linear shallow water model can be interpreted as representing a particular baroclinic mode under vertical normal mode decomposition (Gill 1982, Sect. 9.10). Wajsowicz (1986) and Wajsowicz and Gill (1986) found that the adjustment process of an ocean initially at rest to latitudinal potential temperature gradients was dominated by the first baroclinic mode, with behavior very similar to that obtained with a shallow water model. With global warming, we also expect the response to be dominated by the first baroclinic mode, which can be modelled by a linear shallow water model.

The shallow water model in spherical coordinates used here was developed originally by R. C. Pacanowski, based on the model of Sadourny (1975). The linear C-grid model, with 1/3 degree horizontal resolution, extended from 65°N to 65°S, with an equivalent depth of 0.9 m, hence a gravity wave speed, c, of 3 ms^{-1}. The only friction was Rayleigh damping in the momentum equations, with a damping coefficient of (10 days)$^{-1}$. Since the damping time scale is much less than the period of the Earth's rotation, the equations of motion are still in near geostrophic balance.

The heating of the lower atmosphere due to an enhanced greenhouse effect is proportional to the logarithm of increased greenhouse gases (Manabe et al. 1991). Therefore, an exponential increase of atmospheric greenhouse gases leads to a nearly linear increase in global mean surface temperature, i.e., if $\langle SST\rangle$ is the globally averaged, sea surface temperature, then we would expect $\Delta\langle SST\rangle$, the change in $\langle SST\rangle$ from global warming, to be linearly proportional to the time t. Bryan et al. (1984) show that in the case of a small perturbation of heat, or a neutrally buoyant tracer, the net global flux of heat into an ocean general circulation model obeys the same scaling laws as a simple diffusive model, although the processes are much more complex. This implies that the flux scales as $t^{-1/2}$ in response to a step function increase of $\langle SST\rangle$ at the surface. The total excess heat gained by the ocean is then the integral of the flux, i.e.

$$\text{Total heat} \propto \int \Delta\langle SST\rangle t^{-1/2}\,dt \propto t^{3/2}, \tag{3}$$

(Bryan 1996). The same $t^{3/2}$ law for total heat uptake may be found in the exact solution for a semi-infinite, uniformly conducting media, if the temperature at the upper boundary increases linearly with respect to time (Crank 1975, 2nd Edn., p. 33).

The sea level Eq. (2) contained a source term $q=Ct^{1/2}$, representing the increase of sea level from thermal expansion due to global warming. In the absence of the divergence term in Eq. (2), this form of q causes h' to increase as $t^{3/2}$, as expected from Eq. (3). The distribution of the increasing oceanic surface heat-flux in the coupled-model is shown in Bryan (1996, Fig. 6a). In experiment A, the source was at full value in the northern North Atlantic from 65°N to 60°N, dropping to zero at 50°N by a cosine taper. Outside the northern North Atlantic, the source term was zero. In experiment B, with forcing in the Southern Ocean, the source term again had a cosine shape in the meridional direction, starting from zero at 45°S, peaking at 55°S and dropping to zero at 65°S. The constant C in the source term was chosen so that at year 70 (about the time the atmospheric carbon dioxide had doubled), the global average sea level would have risen by about 15 cm (a value found in the coupled GCM simulation by Bryan 1996).

3 Adjustment to a source in the northern N. Atlantic

The Rossby adjustment problem was introduced by C. G. Rossby as a simple tool to gain insight into how a rotating fluid adjusts towards equilibrium (Gill 1982). A step discontinuity in the sea level of an unbounded fluid initially at rest would adjust, after the passage of Poincaré waves, to a final equilibrium state where the difference in the sea level remained, though the initial sharp front would be widened to a width governed by the Rossby radius of deformation. Later, greater complexities were added to the Rossby adjustment problem to make it more relevant to the ocean. Side walls were introduced by Gill (1976), and bottom topography by Hsieh and Gill (1984). With side walls, the coastal Kelvin wave, which has a major role in the adjustment, eventually turns into a steady, coastally trapped current in the equilibrium state. In order to illustrate in a very simple way the redistribution of pressure caused by high latitude warming, we carry out experiments similar to those of Kawase (1987), who was investigating the outflow of deep water from high latitude source regions.

Figure 1 illustrates the early stages of adjustment from a source of rising sea level in the northern N. Atlantic (experiment A). At 4 months (Fig. 1a), a Kelvin wave had traveled down the east coast of North America and had converted to an equatorial Kelvin wave traveling eastward across the Atlantic. The propagation speeds of the coastal and equatorial Kelvin waves were consistent with the theoretical values for the damped C grid model given by Hsieh et al. (1983) and Ng and Hsieh (1994). At 12 months (Fig. 1b), the equatorial Kelvin wave had moved across the Atlantic, split

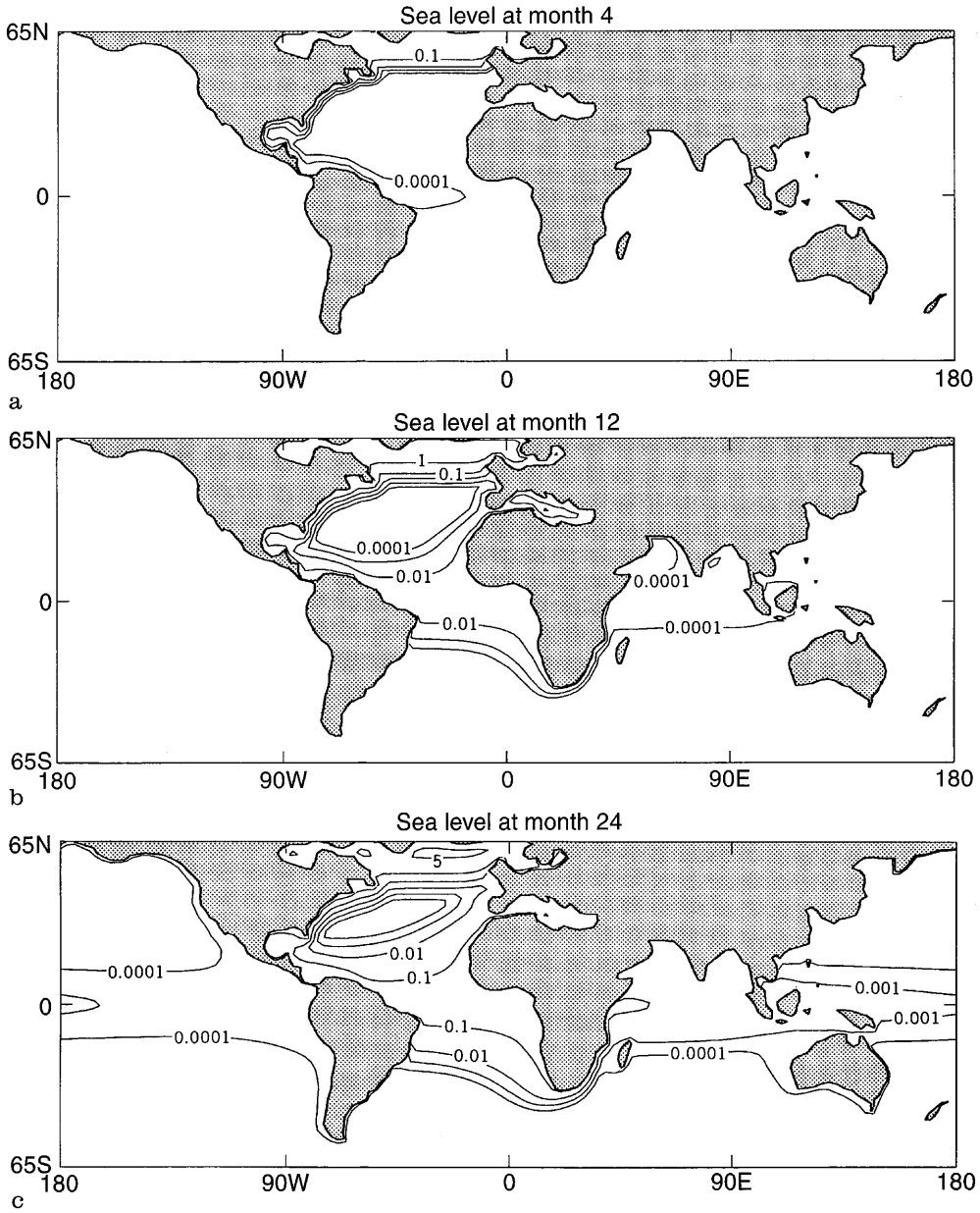

Fig. 1. a Results from the high-resolution reduced gravity model monthly averaged sea level (in cm) at month 4 from the start of experiment A with source in the northern North Atlantic, showing the southward transport of water by the Kelvin wave along the east coast of North America. **b** At month 12 and **c** month 24. Contours levels are: 0.0001, 0.001, 0.01, 0.1, 1 and 5 cm

into coastal Kelvin waves, one moving northward up the coast of Europe, and the other southward, then around the Cape of Good Hope into the Indian Ocean, where it propagated as an equatorial Kelvin wave. The east coast Kelvin waves further radiated westward propagating long Rossby waves with a theoretical phase speed of around $-\beta R^2$, where β is the Coriolis gradient parameter and R the internal Rossby radius. As R increases towards the equator, we expect the westward propagation from the east coast to be faster in the lower latitudes, as indeed observed in Fig. 1b. At 24 months, the equatorial Kelvin wave had traveled across the Pacific Ocean, turning into coastal Kelvin waves along the west coast of North and South America. The Kelvin wave traveling northward along the west coast of North America eventually reached Asia, while the Kelvin wave traveling along the west coast of South America eventually turned around Cape Horn to travel northward along the east coast of South America. Intriguingly, the center of the North Atlantic, despite close proximity to the source region, remained unaffected by the sea level rise after 24 months.

The westward propagating long Rossby waves emitted by the coastal Kelvin waves from the eastern boundary of the Atlantic Ocean began to set up poleward interior flow, which could be inferred from the positive eastward sea level gradient in Fig. 1c (as expected from Stommel and Arons 1960b). As the long Rossby waves arrived at the east coast of South America, poleward boundary currents were set up, as manifested by the sharp sea level gradients in Fig. 1c. For the same reason, when the long Rossby waves arrived at the east coast of North America, one would expect the equatorward boundary flow to weaken slightly. In summary, in the Atlantic, the first stage of the adjustment involved the equatorward western boundary current from the source region first turning into an eastward equatorial current, then transforming into eastern boundary Kelvin waves. In the second stage of adjustment, the propagation of long Rossby waves from the eastern boundary set up the poleward interior flow, and eventually, the cross-equatorial western boundary flow in the Southern Hemisphere, as in Kawase (1987).

At year 70 (Fig. 2), the sea level in the source region, averaging about 90 cm, was much higher than outside. Excluding the source region, the Atlantic Ocean had an average sea level rise of a little over 30 cm, the Indian Ocean, about 15 cm, and the Pacific Ocean, about 12 cm. In the tropics, all three oceans had higher sea level in the west than in the east, due to the eastward propagating equatorial Kelvin waves. The Southern Ocean experienced the least amount of sea level rise, especially between 0 and 70°W, where the sea level rise was only about 1–2 cm, consistent with the small increase in dynamic topography in this region from the coupled model (Bryan 1996, Fig. 3). These comparisons between the models must necessarily be rather qualitative, as the Rossby adjustment problem assumed the total heat input into the world ocean to be concentrated in the northern North Atlantic. The large sea level rise in mid-latitude North Pacific observed in the dynamic topography from the coupled model (Bryan 1996, Fig. 3) but not in the Rossby adjustment model (Fig. 2) suggests its cause to be local heating over the mid-latitude North Pacific.

Stommel and Arons (1960b) examined the steady-state response of an ocean model to deep water formation at high-latitudes balanced by a uniform upwelling over the remainder of the ocean. The theory is examined in more detail by Kawase (1987). In essence, the Stommel and Arons (1960b) model is a shallow water model similar to that used in this study. There is an analogy between the steady state adjustment to a mass source in high-latitudes balanced by a uniform sink in low latitudes envisioned by the Stommel-Arons model and the long term behavior of the present model in which enhanced greenhouse warming introduces a buoyancy source in higher latitudes, which is balanced by a nearly uniform increase in sea level over the remainder of the ocean. In Fig. 2 the sea level contours in the Southern Ocean are tilted in the zonal direction with higher values to the east. This is consistent with a slow, geostrophically balanced, poleward drift, in which the beta effect compensates the stretching of water columns due to a rising sea level. This is the same mechanism of the Stommel-Arons model except that in their case the column stretching is interpreted as an upwelling of deep water balanced by downward diffusion of heat and salinity in the main thermocline.

The coastal currents seen in Fig. 2 are also the counterpart of abyssal western boundary currents in the

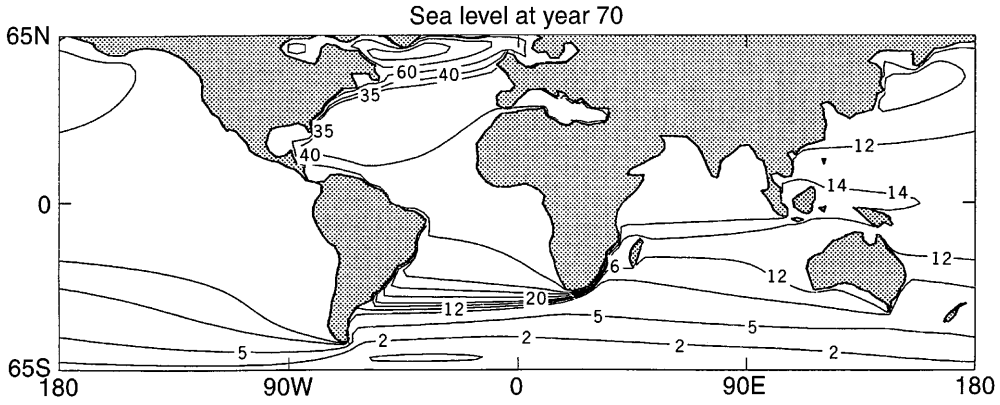

Fig. 2. Annual sea level (in cm) for year 70 in experiment A of the reduced gravity model (North Atlantic source). Contours levels are: 1, 2, 5, 10, 12, 14, 16, 20, 25, 30, 35, 40, 60, 100 and 150 cm

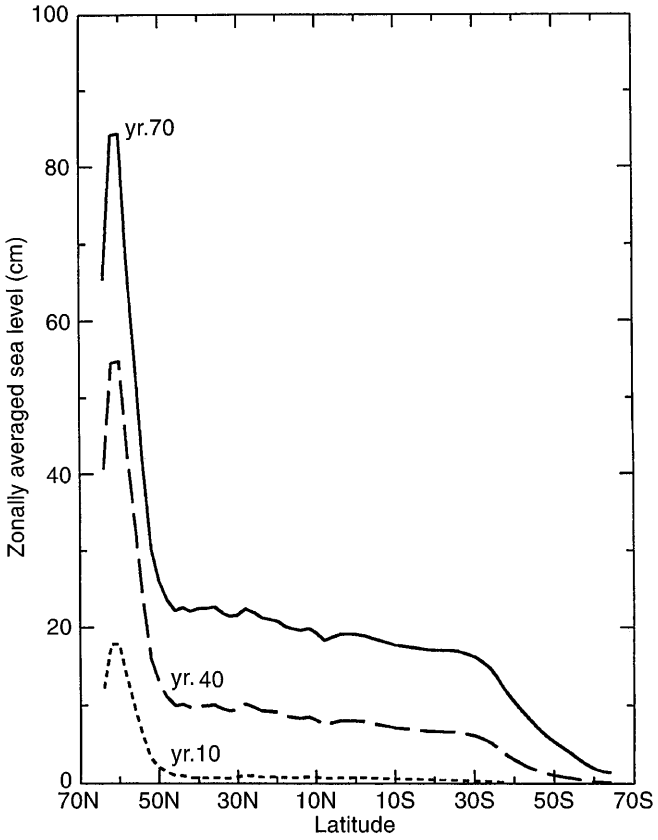

Fig. 3. Zonallyaveraged annual sea level of the reduced gravity model for year 70 (*solid curve*), year 40 (*dashed curve*) and year 10 (*dotted curve*) in experiment A (North Atlantic source)

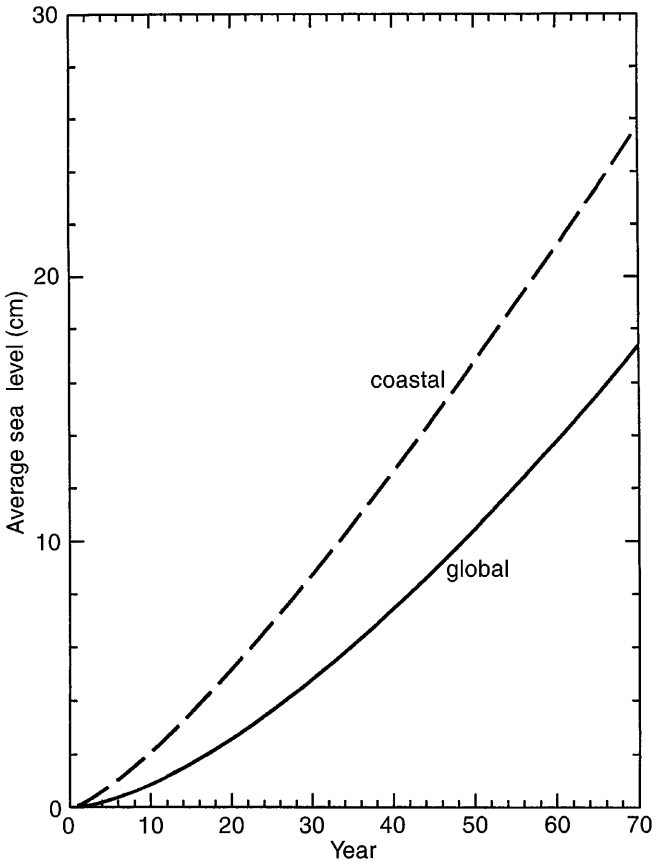

Fig. 4. The reduced gravity model average global sea level (*solid curve*) and average coastal sea level (*dashed curve*) as a function of time during experiment A (North Atlantic source)

Stommel-Arons model. The poleward western boundary current along the east coast of South America was now established. However, as seen from the offshore sea level gradient off the east coast of South America (Fig. 2), this poleward boundary current stopped at 40°S, and was replaced by an equatorward boundary current further south, this being fed mainly by the Kelvin wave from the Pacific turning around Cape Horn (Fig. 1c). At 40°S an eastward jet crosses the Atlantic to the southern tip of Africa, turning into an equatorward boundary current off the southeastern coast of Africa. In general, the Antarctic Circumpolar Current would be slightly enhanced due to the elevated sea level to the north.

The zonally integrated sea level at year 70 (Fig. 3) showed high values at latitudes north of 50°N, a rather flat region from 50°N to 35°S, and a notable decline further south, not unlike that found for the zonally integrated dynamic topography from the coupled model (Bryan 1996, Fig. 4), (though the high sea level north of 50°N in Fig. 3 was essentially only contributed by the North Atlantic).

Estimates of global sea level rise have been based on coastal tidal data (Warrick and Oerlemans 1990), with the assumption that sea level rises similarly in the open ocean. To test the adequacy of such an assumption for our model, we computed in experiment A the average coastal sea level along the world's coastlines and compared it to the average global sea level (Fig. 4). The average coastal sea level was rising much faster than the average global sea level, especially in the early years. The ratio of the average coastal sea level to the global value was 4 in year 1, dropping to 2 in year 20. Hence, there is a danger that the coastal tide gauges may yield a completely inaccurate estimate of the sea level rise associated with global warming, especially during the early stages.

The discrepancy between global sea level and coastal sea level shown in Fig. 4 arose from two factors. One is that baroclinic Kelvin waves hug the coasts and the equatorial wave guide as they propagate out from source regions. The second factor is that some ocean basins have a much lower ratio of coastal area to total area than others. The importance of these two factors can be separated to some extent by the time dependent behavior. In the early stages of adjustment, the effect of Kelvin waves hugging the coast was most important and the ratio of coastal sea level rise to area averaged sea level rise was 4 to 1. However, the Pacific basin has a much lower ratio of coastal area to total area than the Atlantic basin. As adjustment proceeded, Fig. 2 showed that the sea level gradients at the coasts were no longer as tight, and the second factor also became more important.

Within the source region, the distribution of sea level was largely zonally uniform at the early stages due to the zonally uniform source term (Fig. 1a). As found by Wajsowicz and Gill (1986), the adjustment process involved a Kelvin wave transmitting high sea level along the east coast of North America and another Kelvin wave transmitting low sea level into the source region along the west coast of northern Europe and eventually traveling counterclockwise around the source region (Fig. 1b, c). With further adjustment by Rossby waves propagating low sea level information from the coast towards the center of the source region (Wajsowicz 1986), the source region sea level displayed a hump centered just south of Greenland by year 70 (Fig. 2), indicating a clockwise circulation in the source region.

The transfer of excess water from the source region seemed to depend heavily on the coastal current along the east coast of North America. Very little transfer appeared to occur in the open ocean near the source, as we did not have lateral mixing in our sea level equation. Let ω be the frequency of Rossby wave, and k and l be the wave numbers with respect to x and y, respectively. With a small internal Rossby radius at high latitudes, the Rossby wave dispersion relation (Gill 1982, Sect. 12.3)

$$\omega^2 = -\beta k/(k^2+l^2+R^{-2}) \approx -\beta k R^2 \tag{4}$$

yields a negligible meridional group velocity $\partial\omega/\partial l$ and hence little meridional transfer of excess sea level in the open ocean by Rossby waves.

At first sight, it appeared from the sea level contours in Fig. 2 that the added water had mainly stayed within the source region even at year 70. In fact, when the volume was computed, there was almost eight times more water added outside the source region than inside the source region; hence the thin coastal current was fairly efficient in transporting water out from the source region.

To estimate the volume transport via the coastal current, we used Gill's (1976) solution of the Rossby adjustment problem in a rotating channel. Initially, the fluid was motionless but the sea level had a step discontinuity, with the up-channel side being higher by the amount h_0. The adjustment proceeded towards the generation of a coastal current, transporting water away from the high sea level region. When the channel is much wider than the Rossby radius, the rate of volume change in the high sea level region is given by

$$\frac{dV}{dt} = -2cRh_0 \tag{5}$$

where c is the gravity wave speed. If the up-channel side is closed, with an area A, then the excess volume V on the up-channel side is given by $V = Ah_0$. Hence Eq. (5) can be approximately expressed as

$$\frac{dV}{dt} = -V/\tau \tag{6}$$

with the e-folding decay time scale

$$\tau = A/(2c\mathrm{R}) \tag{7}$$

For our problem, $t = 1.25$ years, i.e., an initially high sea level in the source region would decay exponentially with an e-folding time scale of about 1.25 years. With the continuous addition of volume, the excess volume in the source region would be governed by

$$\frac{dV}{dt} = -aV/\tau + bt^{1/2} \tag{8}$$

where b was from the known source, and a, the unknown parameter, allowed the outflow rate along the coastal current to be different from the Gill solution. There were three factors that explained why the outflow rate from Gill's theory could be an overestimate in our situation: (1) there was no step discontinuity in the initial sea level, (2) in the source region, the counter-clockwise propagating low sea level Kelvin wave originating from the eastern boundary eventually traveled around to the western boundary, setting up a clockwise recirculation in the source region, which would diminish the outflow rate, and (3) the gradual rise of sea level outside the source region reduced the sea level difference between the source region and the outside region, hence the outflow rate. If we set $a = 0$ in (8), V and hence the sea level would rise as $t^{3/2}$, as expected from the exponential increase of atmospheric carbon dioxide with time.

An analytic solution of this first-order nonhomogeneous equation could be written in terms of the incomplete gamma function, though it was more straightforward to integrate Eq. (8) with a 4th order Runge-Kutta scheme. Two curves corresponding to $a = 0.25$ and 0.30 were plotted against the observed V in experiment A (Fig. 5). There was good agreement in the basic shapes of the curves in Fig. 5, which all concaved down instead of up as in the global sea level curve in Fig. 4 (which rose as $t^{3/2}$). The fact that the theoretical curves in Fig. 5 had faster sea level rise than observed in the experiment (solid curve) in the early decades, but slower rise in the later decades implied that the outflow term in Eq. (8) with a in the range 0.25–0.3 was too low during early adjustment but too high during later adjustment, consistent with factors (2) and (3) discussed earlier.

There was an additional numerical effect which could cause the coastal current transport to be unrealistically low, resulting in the high sea level in the source region. From Hsieh et al. (1983), we knew that the ill-resolved coastal Kelvin wave in the C-grid tended to be narrower than the continuum solution, in contrast to the Kelvin wave in the B-grid (as used in the ocean component of the coupled model) which tended to be broader and more slowly propagating than the continuum solution. Even with 1/3 degree resolution, the ratio of the grid spacing to the Rossby radius was up to 0.9 in mid- to high-latitudes, hence numerical distortions would be significant. A numerically narrowed Kelvin wave in the C grid could potentially reduce the proper amount of outflow from the source region.

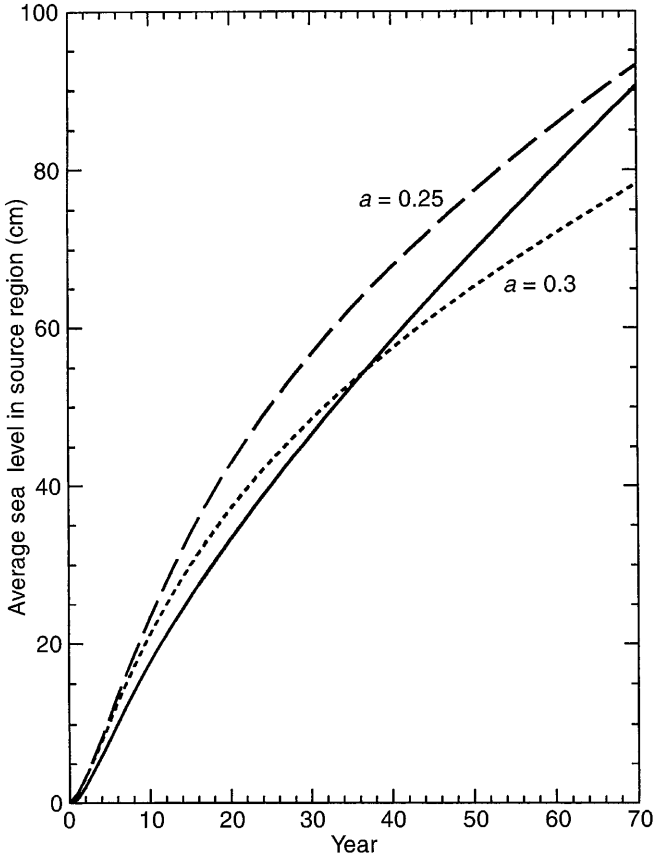

Fig. 5. Average sea level in the source region (*solid curve*) for experiment A (North Atlantic source) of the reduced gravity model, and the theoretical curves calculated by integrating Eq. (8), with $a=0.25$ for the *dashed curve,* and $a=0.3$ for the *dotted curve*

4 Adjustment to a source in the Southern Ocean

In experiment B, the zonally uniform source in the Southern Ocean produced quite different sea level rise in the various oceans. At year 70, the average sea level rise was about 8–9 cm in the Atlantic, about 5 cm in the Indian Ocean and about 3–4 cm in the Pacific (Fig. 6). The relatively strong rise in the Atlantic was due to the more effective coastal wave guide provided by the South American continent which extended much further south than either Africa or Australia. High sea level from the Southern Ocean then traveled along the east coast of South America into the Atlantic. Africa also provided a coastal wave guide for flow into the Indian Ocean and onto the Pacific via equatorial Kelvin waves. As our model truncated the Southern Ocean at 65°S, we could only speculate as to the sea level rise around Antarctica if our model had extended further south. Since much of the excess sea level only extended northward by a few degrees from the zonal source region, we estimated the southward spread to be similarly limited, hence the sea level rise around Antarctica would remain small despite having a source in the 45°S–65°S band. The sea level distribution in the Circumpolar Current region reveal a substantial strengthening of the eastward flow in the northern part of the Southern Ocean and a weakening of the eastward flow in the region close to Antarctica. This type of source acting alone would cause a northward shift of the Circumpolar axis. In general, the sea level in the source region spread much less effectively to other parts of the globe in experiment B than in experiment A. For instance, in the region 50°N–30°S, the average sea level rise at year 70 in experiment B (Fig. 7) was less than a third that in experiment A (Fig. 3). This major difference was due to the lack of adequate coastal boundaries to efficiently transmit excess volume via Kelvin waves from the Southern Ocean to other oceans. The average coastal sea level around the globe was also much lower than the average global sea level in experiment B (Fig. 8), opposite to that observed in experiment A (Fig. 4). This illustrates another danger in using coastal tide gauges to monitor global sea level rise, coastal sea levels around the globe are, in general, oversensitive in responding to the Northern Hemisphere warming but are rather insensitive to Southern Hemisphere warming, with the degree of oversensitivity and undersensitivity being worst during the early stages of global warming.

Figure 2 and Fig. 6, which show the 70 year response for experiments A and B, both show a greater response in the Atlantic sector than the Pacific, which is an apparent discrepancy with the coupled GCM sea level rise shown in Bryan (1996, Figs. 3, 4). However,

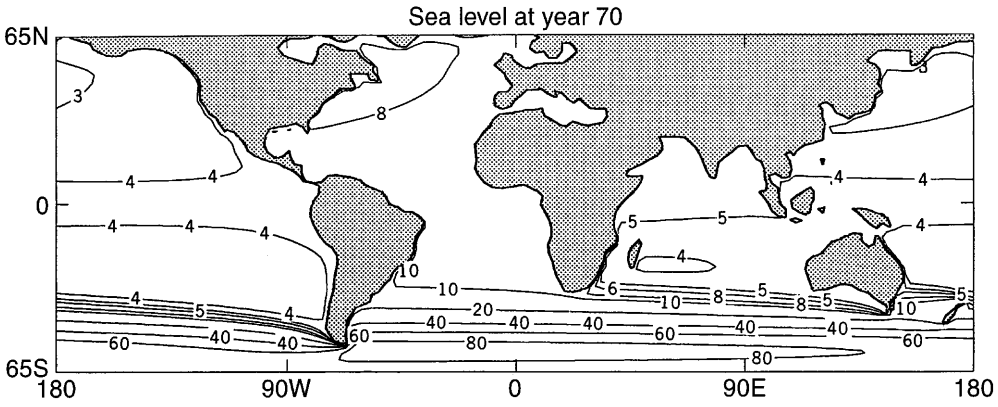

Fig. 6. Annual sea level (in cm) for year 70 in experiment B of the reduced gravity model (Southern Ocean source), with the source located in the Southern Ocean. Contour levels are: 3, 4, 5, 6, 8, 10, 20, 40, 60 and 80 cm

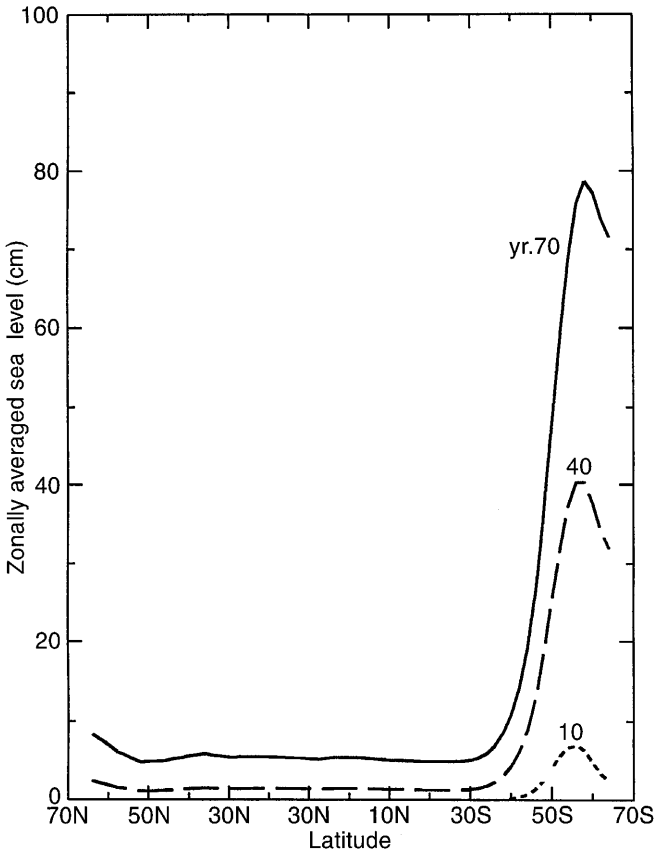

Fig. 7. Zonally averaged annual sea level of the reduced gravity model for year 70 (*solid curve*), year 40 (*dashed curve*) and year 10 (*dotted curve*) in experiment B (Southern Ocean source)

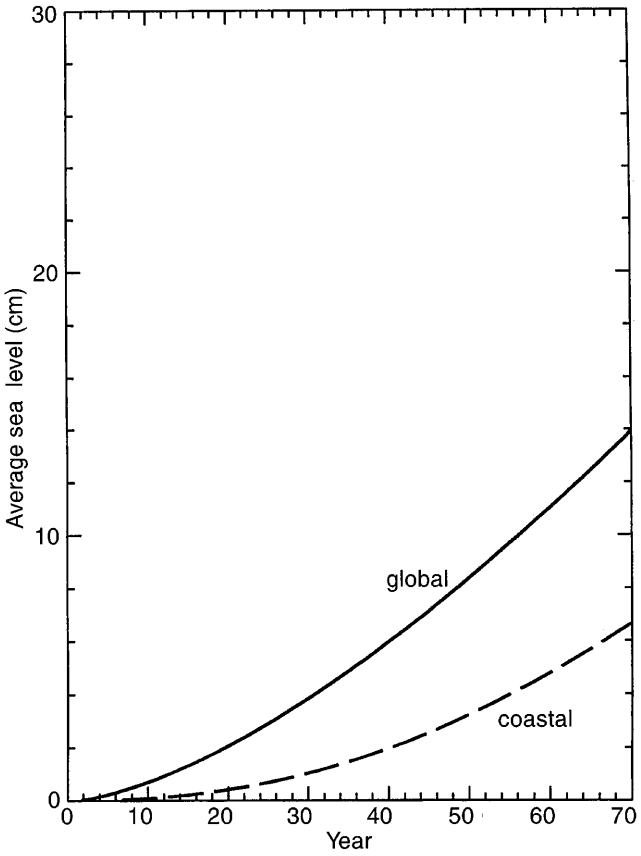

Fig. 8. Average global sea level (*solid curve*) and average coastal sea level (*dashed curve*) as a function of time during experiment B (Southern Ocean source) of the reduced gravity model

Bryan (1996, Fig. 6a) shows that global heat input is significantly larger between 0°–40°S than the Atlantic heat input. This shows that there is a significant heat input in the Indian-Pacific sector which is not represented in experiments A or B, which could account for part of the discrepancy.

5 Summary and conclusions

To study the effects of the redistribution of heat by a spindown of the thermohaline circulation associated with greenhouse warming, we examined the Rossby adjustment problem in a simple shallow-water model of much higher horizontal resolution than the coupled GCM of Bryan (1996). We examined the roles of coastal and equatorial Kelvin waves and Rossby waves in spreading the rising sea level away from the source regions of high heat input. In experiment A, where the source region was in the northern North Atlantic, the excess volume was transferred out of the source region mainly by a coastal current along the east coast of North America, bending eastward at the equator as an equatorial Kelvin wave, which generated poleward Kelvin waves on the eastern boundary. As the Kelvin wave continued around the Cape of Good Hope, the high sea level was transmitted into the Indian Ocean and then into the Pacific. In the Atlantic, westward propagating long Rossby waves originating from the eastern boundary set up poleward interior flow, as well as cross-equatorial western boundary flow southward along the east coast of South America. In experiment B, where the source region was in the Southern Ocean, the lack of adequate coastal wave guides hindered the transport of excess volume out of the source region.

Coastal sea level was examined as a signature of global sea-level rise. In our idealized model, coastal sea level around the globe responded differently to the sea level rise from the two source regions, being overly sensitive to the rise in the northern North Atlantic, and rather insensitive to the rise in the Southern Ocean, with the degree of oversensitivity and undersensitivity worst during the early stages of global warming. These experiments cast doubt on the assumption that the coastal tide gauges alone can provide a reasonable estimate of the global sea level rise expected from an enhanced greenhouse warming.

There were two puzzling features of the sea level rise predicted by the coarse resolution coupled ocean-atmosphere climate model of Bryan (1996). One feature was the time scale of the ocean circulation "spindown", which weakened the normal poleward transport of heat. The second feature was the marked delay in sea level rise in the Southern Ocean in the imme-

diate vicinity of Antarctica. The simple, shallow water model provided some insight on both of these features. It showed that the time scale of response was not controlled by the speed of coastal Kelvin waves, which rapidly transmitted signals around the globe, but by a much slower process of transport in coastal jets which linked high and low latitudes. Coastal jets could not penetrate into the Southern Oceans south of Cape Horn, which explained the slow response of sea level in the extreme poleward parts of the Southern Ocean to buoyancy sources to the north.

Our linearized shallow water calculations were intended to provide some insights into the mechanisms of non-equilibrium sea level rise in response to buoyancy sources. The schematic nature of the source regions did not allow a detailed comparison of the sea level rise shown in the calculations of Bryan (1996), which showed the effects of a much more widely distributed buoyancy source due to greenhouse warming. In Bryan (1996) enhanced buoyancy input north of the Antarctic Circumpolar Current gave rise to very little sea level rise in the Southern Ocean south of the Current. In the present study, the effects of a source region in the Southern Ocean were largely trapped locally with very little spreading to the north. The linearized shallow water model showed that the geometry of the Southern Ocean was a formidable barrier for communication by Kelvin and Rossby waves with the rest of the World Ocean. In the lower resolution, but more realistic model used by Bryan (1996) other factors such as the great change in thermocline depth across the Circumpolar Current and the Current itself may come into play. Another uncertainty that comes into the interpretation of the model results is the possible role of mesoscale eddies in a more complete model. A key factor in the timescale of the response shown in this study is the constraint on adjustment played by the very narrow coastal currents set up by Kelvin waves. In a background of a variable thermocline depth and vigorous mesoscale eddies it is not clear whether coastal or equatorial Kelvin waves act in the same way. The present study must be considered only the first step in the study of what may be called the "global ocean Rossby adjustment problem". There is a clear need for continuing this work with more realistic, higher resolution, three-dimensional ocean circulation models.

Acknowledgements. The authors are grateful for the essential assistance received from K. Dixon, R. Pacanowski and R. J. Stouffer. Comments on a draft of the manuscript by R. J. Stouffer, K. Hamilton and V. Larichev were very helpful. W. Hsieh was supported by research grants from the Natural Sciences and Engineering Council of Canada and the University of British Columbia Killam Faculty Research Fellowship. The authors are indebted to C. Raphael, J. Varanyak and W. Marshall for their assistance in preparing the figures and the manuscript.

Appendix. The linearized shallow water equations

The linearlized shallow water equations are:

$$\partial_t \boldsymbol{u}' + f\boldsymbol{k}\times\boldsymbol{u}' + g\gamma\nabla h' = -\mu\boldsymbol{u}' \tag{A1}$$

and

$$\partial_t h' + \nabla\cdot(\overline{\boldsymbol{u}}h' + \boldsymbol{u}'\overline{h}) = q' \tag{A2}$$

where the overbar denotes mean quantities and the prime denotes perturbation quantities. Here nonlinear effects in the momentum equation are omitted, but the interaction of the upper layer thickness field with the mean flow is retained in (A2). If (A2) is written out,

$$\partial_t h' + \overline{\boldsymbol{u}}\cdot\nabla h' + \boldsymbol{u}'\cdot\nabla\overline{h} + \overline{h}\nabla\cdot\boldsymbol{u}' + h'\nabla\cdot\overline{\boldsymbol{u}} = q'. \tag{A3}$$

Assume $\boldsymbol{u}'$, h' are O( ) quantities with respect to the O(1) quantities, $\overline{\boldsymbol{u}}$, $\overline{h}$. Also assume $\overline{\boldsymbol{u}}$ and $\boldsymbol{u}'$ are approximately geostrophic to O(δ) and O(δ), respectively. Ignoring terms of O(δ), one can show that the second and third terms on the left hand side of (A3) cancel each other, while the ratio of the fifth term to the fourth term in (A3) is

$$R \approx \frac{h'\overline{h}_x}{\overline{h}h'_x} \approx \frac{h'\overline{v}}{\overline{h}v'}. \tag{A4}$$

As $\overline{h}$ is associated with the entire thickness of the thermocline, not just the variations of thermocline depth associated with the mean circulation, hence

$$\frac{h'}{\overline{h}} \ll \frac{v'}{\overline{v}}. \tag{A5}$$

As R would then be expected to be small, only the first and the fourth terms on the left hand side of (A3) are retained to yield Eq. (2) (with primes dropped). This scaling breaks down, of course, if the full variations of thermocline thickness in regions like the Antarctic Circumpolar Current are taken into account.

References

Bryan K (1996) The steric component of sea level rise associated with enhanced greenhouse warming: a coupled GCM study. Clim Dyn (this issue)

Bryan K, Komro FG, Rooth C (1984) The ocean's transient response to global surface temperature anomalies. In: Climate processes and climate sensitivity, Geophysical Monograph 29, Maurice Ewing Volume 5, pp. 29–38

Crank J (1975) The mathematics of diffusion. Clarendon Press, Oxford, 2nd Edn.

Gill AE (1976) Adjustment under gravity in an rotating channel. J Fluid Mech 77:603–621

Gill AE (1982) Atmosphere-ocean dynamics. Academic Press, Orlando, USA

Hsieh WW, Gill AE (1984) The Rossby adjustment problem in a rotating, stratified channel, with and without topography. J Phys Oceanogr 14:424–437

Hsieh WW, Davey MK, Wajsowicz RC (1983) The free Kelvin wave in finite-difference numerical models. J Phys Oceanogr 13:1383–1397

Kawase M (1987) Establishment of deep ocean circulation driven by deep-water production. J Phys Oceanogr 17:2294–2317

Manabe S, Stouffer RJ, Spelman M, Bryan K (1991) Transient responses of a coupled ocean-atmosphere model to gradual changes of atmospheric carbon-dioxide, Part I: annual mean response. J Clim 4:785–818

Ng M, Hsieh WW (1994) The equatorial Kelvin wave in finite-difference models. J Geophys Res 99:14173–14185

O'Brien JJ, Parham F (1992) Equatorial Kelvin waves do not vanish. Mon Weather Rev 120:1764–1766

Philander SG (1990) El Niño, La Niña, and the Southern Oscillation. Academic Press. San Diego, USA

Sadourny R (1975) Compressible model flow on the sphere. J Atmos Sci 32:2103–2110

Stommel H, Arons AB (1960a) On the abyssal circulation of the world ocean – I. Stationary planetary flow patterns on a sphere. Deep Sea Res 6:140–154

Stommel H, Arons AB (1960b) On the abyssal circulation of the world ocean – II. An idealized model of the circulation pattern and amplitude in oceanic basins. Deep Sea Res 6:217–233

Wajsowicz RC (1986) Adjustment of the ocean under buoyancy forces. Part II: the role of planetary waves. J Phys Oceanogr 16:2115–2136

Wajsowicz RC, Gill AE (1986) Adjustment of the ocean under buoyancy forces. Part I: the role of Kelvin waves. J Phys Oceanogr 16:2097–2114

Warrick R, Oerlemans J (1990) Sea level rise. In: Climate change: the IPCC Assessment, pp 261–279